JOURNAL OF MATERIALS SCIENCE **40** (2005) 6157–6168

Nondestructive detection of fatigue damage in austenitic stainless steel by positron annihilation

PETRA SCHAAFF, UWE HOLZWARTH
European Commission, Joint Research Centre,Institute for Health and Consumer Protection, Via E. Fermi 1 (T.P. 500), I-21020 Ispra (VA), Italy
E-mail: petra@schaaff.net

Published online: 8 September 2005

Austenitic stainless steel specimens have been examined by positron-lifetime measurements at various stages until failure during fatigue tests at constant stress or plastic strain amplitudes. A positron-source-detector assembly has been mounted on the servohydraulic testing machines that allowed truly non-destructive positron annihilation studies without removing the specimens from the load train. Positrons were generated by a $^{72}Se/^{72}$ As source with a maximum activity of 0.9 MBq (25 μCi). The average positron lifetime has been determined by a $\beta^+ - \gamma$-coincidence applying a simplified data evaluation procedure. Under constant stress or plastic strain amplitudes early stages of fatigue damage could be detected. The strong increase of the average positron lifetime already during the first 10% of fatigue life could be related to the fatigue life of the specimens. Issues of lifetime prediction by positron annihilation measurements are discussed.

1. Introduction

The non-destructive characterization of damage in materials and components subjected to alternating mechanical load and the assessment of residual service lifetime are still a serious engineering problems [1, 2]. The evolution of fatigue damage in metals is a highly complex process of microstructure change involving atomic defects, dislocations, grain boundaries and depending on the composition and the pre-treatment of the material also precipitates and phase transitions as well as interactions between all these defects. The evolution of the densities of atomic defects, their agglomerates and jogs on dislocations is superimposed [3, 4] on the evolution of dislocation cells or peculiar dislocation patterns like persistent slip bands [5, 6]. This leads to a modulation of the dislocation density by a factor of 10^2 to 10^4 (typically from 5×10^{12} m^{-2} up to 1.4×10^{17} m^{-2}) on a length scale of a few μm [4, 7]. However, non-destructive methods for field applications that are sufficiently sensitive for the detection of early stages of fatigue-induced microstructure changes are still missing [2]. Most of the commonly applied techniques become sensitive to fatigue damage shortly before failure when microscopic cracks are already present and crack coalescence and accelerated crack growth start. More sensitive methods like X-ray line broadening require polished surfaces, and Barkhausen noise is confined to ferromagnetic materials. X-ray diffraction, eddy currents or ultrasound methods measure the effect of dislocations, atomic defects, defect clusters or microcracks on physical properties like interlattice plane distance, electrical resistivity or sound propagation, respectively. On the other hand, positron annihilation is highly sensitive to open-volume defects such as lattice vacancies or dislocations and can detect them at such low densities that they hardly start to measurably change the material properties measured by other techniques. In this sense, positron annihilation is a more direct and hence more sensitive method to measure damage.

The high sensitivity of positron annihilation to vacancy-like defects in crystalline matter is well known (see the reviews [8–11]). The annihilation radiation of positrons contains information on the local electron density and the electron momentum distribution at the positron trapping sites and is therefore useful to characterize the size of open-volume defects and their chemical environment in dilute concentration. Whenever a positron gets trapped in an open-volume defect its annihilation rate is proportional to the local electron density. The larger the defect the lower is the local electron density and the more the lifetime of the positron increases. Each type of open-volume defects has its individual positron lifetime, and positron lifetime spectroscopy can be used to identify and quantify defects in materials. However the co-existence of various types of potentially positron-trapping defects (like dislocations, jogs, vacancies, multiple vacancies and vacancy clusters of various size and configuration) that are produced simultaneously in fatigue and the corresponding complexity of positron diffusion, trapping and annihilation precludes the identification of individual trap lifetimes within the experimental limitations in field

0022-2461
DOI: 10.1007/s10853-005-3163-5

TABLE I Chemical composition of stainless steel AISI 316 L according to supplier certificate

Elements	C	Si	Mn	Ni	Cr	Mo	S	P	Fe
Wt%	0.018	0.582	1.676	11.13	17.38	2.151	0.002	0.021	67.04
at-%	0.08	1.15	1.69	10.53	18.57	1.24	0.01	0.04	66.68

applications. The present paper deals with the question whether a simplified evaluation procedure limited to the evaluation of the average positron lifetime could be employed for nondestructive assessment of fatigue damage and residual lifetime assessment in an engineering material.

Several attempts have been reported in literature to develop systems for nondestructive testing using positron-lifetime measurements by a $\beta^+-\gamma$-coincidence technique [12, 13] or positron annihilation lineshape analysis [13–18]. The experimental set-up of a ^{72}Se/^{72} As positron generator for nondestructive measurements used in the present paper has already been presented [12] and also preliminary results on in-situ positron-lifetime measurements during fatigue of stainless steel AISI 316 L [19].

The large amount of measurements in the present paper has been economically affordable only due to the truly nondestructive technique that avoids time consuming specimen preparation. Therefore we could focus on aspects of experimental reproducibility. So far, most positron annihilation studies on fatigue present only single sets of experiments. And in some publications different stages of fatigue life under nominally identical fatigue parameters are established and probed in different specimens (e.g. [13, 20]).

The complex of fracture mechanics is not touched in the present publication. We consider crack growth and crack propagation as phenomena of late fatigue life that can be examined by the already applied nondestructive testing tools.—It will be shown that measurements of the average positron lifetime can reveal beginning fatigue damage in austenitic stainless steel. Moreover, positron lifetime measurements in early fatigue life can provide an early rough indication on residual service life in laboratory experiments.

2. Experimental procedures

2.1. Material and specimen preparation

The present investigation deals with the low-carbon austenitic stainless steel type AISI 316 L. The fatigue behaviour of this material has extensively been studied for nuclear energy applications including TEM studies [21–23]. It remains a single phase austenitic material under all application conditions relevant to this study. Therefore, no deformation induced phase transformations need to be considered in the evaluation of positron-lifetime measurements.

Stainless steel AISI 316 L was supplied by Creusot-Loire in plates of 1 × 2 m and 30 mm thickness. The material composition is specified in Table I. The plates had been hot rolled, solution annealed at 1050°C for 30 min and then quenched by submersion in cold water. Metallography revealed a ferrite content of about 1% only. Ferrite is mainly arranged in stringers parallel to the rolling direction of the material. The average grain size of the material has been determined by the linear intercept method according to ASTM E112 [24] and was 40–50 μm. From these plates bars of 30 × 30 × 170 mm were cut by spark erosion and cylindrical fatigue specimens with tangentially blending fillets between the gauge length and the gripping parts were machined. The specimen axis was parallel to the rolling direction. The tensile properties are characterized by an elastic limit $\sigma_{0.2} = (244 \pm 6)$ MPa, an ultimate tensile strength $\sigma_{UTS} = (595 \pm 13)$ MPa and a uniform plastic strain of (46 ± 5)% [25].

Specimen shapes, the fabrication process by machining and the execution of the fatigue tests complied with the ASTM Standards E 466 and E 606 [24]. The resulting surface finish on the gauge length exhibited a maximum roughness of 0.2 to 0.25 μm. Two types of specimen geometries were used since the fatigue testing systems were equipped with different specimen grips. Specimens for the experiments on the Instron servohydraulic testing system type 1273 and on the MTS system 810 with maximum load capacity of 250 kN were of type A in Fig. 1. The specimens used on the MTS system 810 with maximum load capacity of 50 kN were button headed specimens of type B (cf. Fig. 1).

In spite of solution annealing and quenching from 78% of the melting temperature (1425°C) of stainless steel AISI 316 L [26], the residual concentration of vacancies was low because the low thermal conductivity of stainless steel (13.95 Wm^{-1} K^{-1} ([26])) strongly limits the cooling rate that can be achieved by water quenching in the center of 30 mm thick plates where the specimens stem from. The concentration of vacancies in a Fe-Cr-Ni alloy after quenching from 1050°C has been estimated by Wang *et al.* [27] to be about 10^{-6}.

2.2. Cyclic deformation—Fatigue

Symmetric push-pull fatigue experiments ($\sigma_{min}/\sigma_{max} = -1$) were performed under load control at nominal stress amplitudes in the range between 220 and 290 MPa with a sinusoidal command wave. The cycling frequency was 10 Hz. For the present material and testing conditions the fatigue limit, defined as the stress amplitude where 50% of the specimens reach 1 × 10^7 cycles without failure was found to be 225 MPa [25].

ε_{tot} is calculated from the elongation Δl along a segment of the length $l_0 = 10$ mm in the center of the gauge length according to $\varepsilon_{tot} = \Delta l/l_0$. l_0 was determined by the dimension of the MTS clip-on extensometer. The elastic part ε_{el} of the total strain ε_{tot} can be calculated from the stress σ and the Young's modulus E.

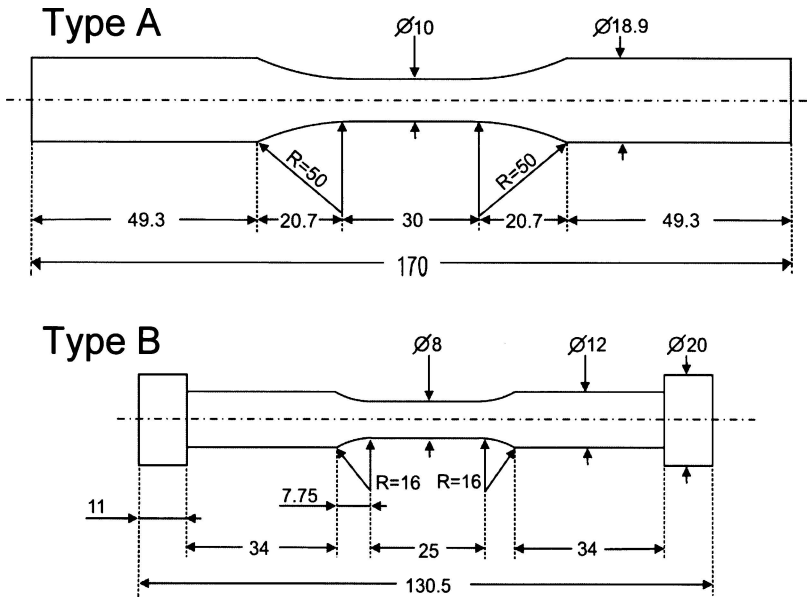

Figure 1 Specimen shapes Type A and Type B used for the fatigue experiments.

The plastic strain ε_{pl} has been calculated on-line from the simultaneous measurement of the total strain ε_{tot} and the stress σ according to

$$\varepsilon_{pl} = \varepsilon_{tot} - \varepsilon_{el} = \varepsilon_{tot} - \frac{\sigma}{E}. \quad (1)$$

Constant plastic strain rate $\dot{\varepsilon}_{pl}$ has been assured by using a triangular command wave for ε_{pl}. Strain-controlled fatigue experiments ($\varepsilon_{pl,\,min}/\varepsilon_{pl,\,max} = -1$) were performed for plastic deformation amplitudes in the range between 1×10^{-4} and 5×10^{-3} with a frequency of 0.5 Hz.

For simplicity, from now on, σ and ε_{pl} shall denote the applied stress amplitude and the applied plastic strain amplitude, respectively.

2.3. Positron lifetime measurements

The fatigue machines have been equipped with a mobile positron beam to perform positron-lifetime measurements without removing the specimen from the load train. Fig. 2 gives an impression on the modification to the load frame and the experimental set-up is presented in Fig. 3. The system was mounted and adjusted in a way to measure always on the same site in the center of the gauge length. Fatigue cycling was stopped for positron-lifetime measurements after 100, 200, 500, 1000, 2000, 5000, 10000 cycles and so on in logarithmic sequence. The last measurements were performed after failure of the specimens.

The production of the miniaturized positron sources used for the present experiments was already described in detail elsewhere [12, 28]. A ^{72}Se/^{72}As generator with a maximum initial activity of about 25 μCi ($\approx$0.9 MBq) was used as positron source. The ^{72}Se was vapour deposited inside a small gold cylinder of 0.6 mm inner diameter acting as beam collimator. The gold cylinder was integrated in the tip of a plexiglass light guide on top of a photomultiplier tube and covered with a plastic scintillator which produces a scintillation start signal only for those positrons that are emitted in the direction towards the specimen under examination. The set-up was shielded against light by a 12 μm thick aluminium foil. A specimen in a distance of 3 mm from the tip of the collimator was subjected to positron irradiation in an area of 3.6 mm in diameter. The stop signal was delivered by a BaF_2 crystal after registration of the 511 keV annihilation quanta. Signal processing was done by a fast-slow coincidence measurement as described earlier [12, 28]. The electronic equipment was housed in a cabinet kept at constant temperature of (20 $\pm$ 0.5)°C.

^{72}As emits two positron spectra with maximum energies of 2.5 MeV and 3.3 MeV [29]. Estimating the most probable positron energy from 1/3 of E_{max} and subtracting an energy loss of 150 keV for the passage of the plastic scintillator, gives a penetration depth of 370 and 550 μm into stainless steel for the 2.5 and 3.3 MeV spectra, respectively. The positron annihilation data obtained in this way are more representative for the bulk properties of a material than those obtained by the classical methods with ^{22}Na with a maximum positron energy of only 544 keV. Compared with the sandwich technique using a ^{22}Na source and a γ-γ-coincidence the present technique exploits a much smaller solid angle. The effect on count rate is however largely compensated by the higher efficiency of the β-γ-coincidence and the higher (initial) source strength of the ^{72}Se/^{72}As generator.

The ^{72}Se/^{72}As generator offers the possibility to register simultaneously a prompt γ-photon of the 835 keV emitted by ^{72}Ge and to monitor the stability of the detection system and its time resolution. The time resolution of the instrument has been determined as the full width half maximum of the 835 keV prompt line. Alternatively, a Gaussian curve has been fitted to the prompt line. Both methods yield a time resolution of (230 $\pm$ 5) ps.

For the positron-lifetime measurements the cyclic deformation has been paused and the specimens have been shielded with plexiglass that captured all positrons

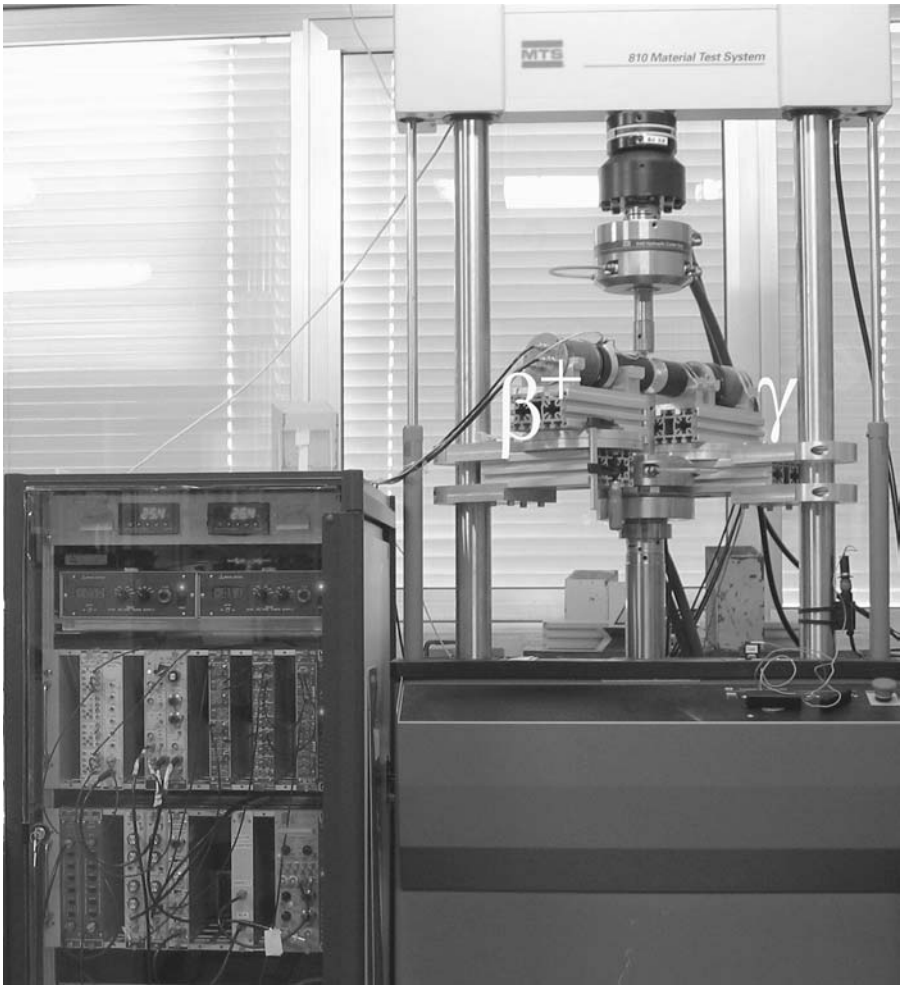

Figure 2 Integration of the β^+ and γ detectors in the load train of a servohydraulic testing machine. The photo multiplier tubes are magnetically shielded in a mumetal cylinder. The positron generator is integrated in the tip of the light guide of the β^+-detector. The 511 keV annihilation photons are detected in a BaF_2 scintillator on top of the second photo multiplier (γ) (see also Fig. 3). The nuclear electronics is housed in a temperature stabilized box left to the load frame.

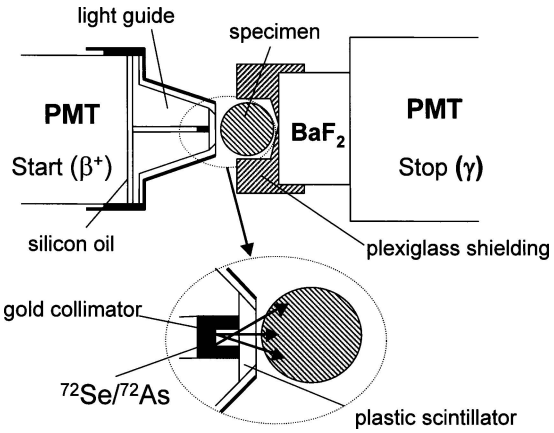

Figure 3 Set-up of the positron lifetime spectrometer as described in Section 2.3.

missing the specimen or being reflected from its surface. The average positron lifetime in plexiglass of about 1500 ps is sufficiently different from the average positron lifetimes expected in a metal of 100–200 ps that an easy background correction can be performed by weighted subtraction of a plexiglass reference spectrum. Reference spectra have been recorded using a plexiglass dummy instead of a steel specimen in the load train. The weighting factor has been determined from the ratio of counts in a window of the spectrum, in which the spectrum was determined by very long-lived contributions only, and the counts in the same window in the reference spectrum. For this background correction the width of the windows and their position with respect to the center of the annihilation spectra were identical. This method corrects also the annihilation events of low energy positrons in the scintillation start detector and the aluminium foil shielding the photomultiplier tube from daylight.

Before correction each spectrum contained 1.1×10^6 coincidence events. The required acquisition time increased from initially about 20 min to more than 2.5 h after 4 weeks due to the 8.4 days half-life of the $^{72}Se/^{72}As$ generator. Typically 55–60% of these events were lost by the weighted subtraction of the reference spectrum. The average positron lifetime has then been evaluated by a weighted linear regression to the linear part of the spectrum (in logarithmic presentation). The statistical error of the fits was less than 1 ps. The overall accuracy of τ_{av} is however ± 3 ps due to the reproducibility of repeated recording of positron lifetime spectra of a reference specimen in the same microstructure state and due to slight differences in the positron lifetime values when minimizing the statistical error by varying the position of the windows

TABLE II Data summary of stress-controlled experiments: applied stress amplitude σ, fatigue life N_f, initial average positron lifetime $\tau_{av}(0)$, average positron lifetime at failure $\tau_{av}(N_f)$ and its increase until failure $\Delta\tau_{av}(N_f)$. Analogously, for experiments stopped after N_s cycles the average positron lifetime $\tau_{av}(N_s)$ and its increase $\Delta\ \tau_{av}(N_s)$ until N_s are given. The specimen shape refers to Fig. 1

Label	σ in MPa	N_f	N_s	$\tau_{av}(0)$ in ps	$\tau_{av}(N_f)$ in ps	$\tau_{av}(N_s)$ in ps	$\Delta\ \tau_{av}(N_f)$ in ps	$\Delta\ \tau_{av}(N_s)$ in ps	Specimen shape
A220	220		650000	129		127		2	Type A
A230	220		10000000	130		151		19	Type A
A240	240		2090000	131		160		29	Type A
B240	240	3353570		129	155		26		Type A
C240	240		500000	120		143		23	Type A
D240	240		1000000	119		131		12	Type A
A250	250	300000		133	172		39		Type A
B250	250	687000		131	163		32		Type A
C250	250	140226		112	141		29		Type A
D250	250	145621		110	146		26		Type A
E250	250		100000	125		147		22	Type B
F250	250	802300		125	146		21		Type B
G250	250	77635		120	152		32		Type B
H250	250	179916		n.a.					Type B
I250	250	291930		n.a.					Type B
A260	260	80000		127	170		43		Type A
B260	260	44967		111	145		34		Type A
A270	270	23000		125	169		44		Type A
B270	270	25000		131	160		29		Type A
C270	270	23000		126	168		42		Type A
D270	270	23000		138	186		48		Type A
E270	270		3000	121		142		21	Type A
F270	270		15000	123		160		37	Type A
G270	270	45349		120	150		30		Type B
H270	270	21037		129	160		31		Type B
A290	290	13000		123	176		53		Type A

for background correction and the weighted linear regression.

A decomposition of the average positron lifetime into different components has not been performed, in order to avoid uncertain assumptions on the type and number of relevant positron traps and to keep the evaluation procedure as simple as described.

3. Results

3.1. Overview on stress- and strain-controlled experiments

All performed stress- and strain-controlled experiments are presented in the Wöhler plot in Fig. 4. Experiments stopped before failure are marked with open symbols. Experimental details are compiled in Tables II and III for stress- and strain-controlled experiments, respectively.

In Figs 5 and 6 the evolution of the average positron lifetime during stress- and strain-controlled fatigue experiments on stainless steel AISI 316 L is presented, respectively. The error bars in Figs 5 and 6 denote the accuracy of the measurement (± 3 ps). In order not to overload the figures, error bars are presented for every second experiment only. In order to keep a logarithmic scale for the number of fatigue cycles N the average positron lifetime $\tau_{av}(0)$ in the undeformed initial state at $N = 0$ is reported at $N = 10^0$. Lines presented in the figures are eye guides to improve apprehension of the data. Since no electrolytical polishing or gentle grinding has been applied after the final machining of the specimens, $\tau_{av}(0)$ exhibits a scatter of (129 ± 5) ps, (110 ± 3) ps and (120 ± 5) ps for the specimen batches

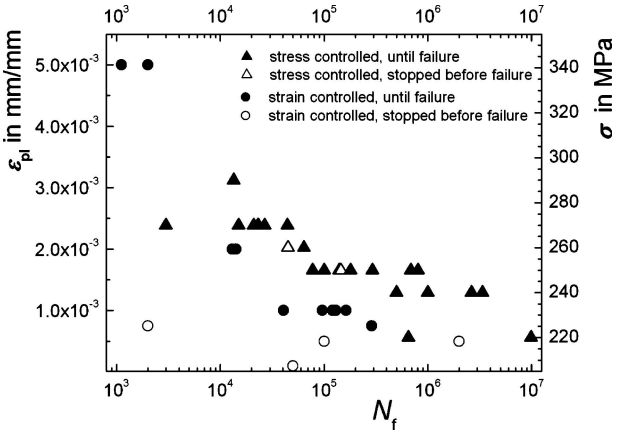

Figure 4 Wöhler plot representing all stress- and strain-controlled experiments, as stress and strain amplitude, right- and left-hand side, respectively, versus fatigue life given by the number of load cycles until failure N_f (filled symbols). Open symbols denote experiments stopped before failure.

used on the systems Instron 1273, MTS 810 (250 kN) and MTS 810 (50 kN), respectively, as indicated in Tables II and III. Plastic deformation of a surface layer by machining could be revealed by positron annihilation up to a depth to 5 mm below the surface [30]. The scatter of the initial average positron lifetime $\tau_{av}(0)$ was usually larger than the accuracy of the average positron lifetime measurement of ± 3 ps. In order to check the influence of the scatter of $\tau_{av}(0)$ on the information to be derived from our experiments, preliminary results had been presented as the increase of the average positron lifetime, $\Delta\ \tau_{av}(N) = \tau_{av}(N) - \tau_{av}(0)$ with respect to their start value $\tau_{av}(0)$ versus the number of load cycles [19]. On the basis of the much larger

TABLE III Data summary of strain-controlled experiments: applied plastic strain amplitude ε_{pl} in mm/mm, fatigue life N_f, initial average positron lifetime $\tau_{av}(0)$, average positron lifetime at failure $\tau_{av}(N_f)$ and its increase until failure $\Delta\,\tau_{av}(N_f)$. Analogously, for experiments stopped after N_s cycles the average positron lifetime τ_{av} (N_s) and its increase $\Delta\,\tau_{av}$ (N_s) until N_s are given. The specimen shape refers to Fig. 1

Label	ε_{pl} in mm/mm	N_f	N_s	$\tau_{av}(0)$ in ps	$\tau_{av}(N_f)$ in ps	$\tau_{av}(N_s)$ in ps	$\Delta\,\tau_{av}(N_f)$ in ps	$\Delta\,\tau_{av}(N_s)$ in ps	Specimen shape
A1E4	1×10^{-4}		50000	118		118		0	Type B
A5E4	5×10^{-4}		1000000	113		146		33	Type B
B5E4	5×10^{-4}		100000	125		136		11	Type B
C5E4	5×10^{-4}		2000000	113		143		30	Type A
A75E4	7.5×10^{-4}	278163		107	139		32		Type A
B75E4	7.5×10^{-4}		2000	113		145		32	Type A
A1E3	1×10^{-3}	40724		113	145		32		Type B
B1E3	1×10^{-3}	120500		119	139		20		Type B
C1E3	1×10^{-3}	163775		125	148		23		Type B
D1E3	1×10^{-3}	130220		115	158		43		Type B
E1E3	1×10^{-3}	95945		111	146		35		Type B
A2E3	2×10^{-3}	14141		114	148		34		Type B
B2E3	2×10^{-3}	13007		126	152		26		Type B
A5E3	5×10^{-3}	1120		132	162		30		Type B
B5E3	5×10^{-3}	2010		121	158		37		Type B

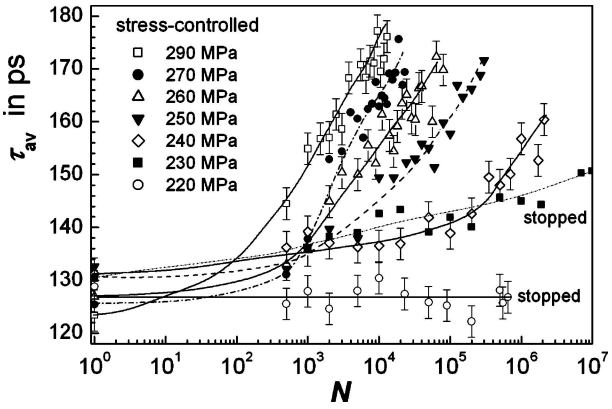

Figure 5 Evolution of the average positron lifetime τ_{av} with the number of stress-controlled load cycles N for different applied stress amplitudes σ given in MPa (A-series: A290, A270, A260, A250, A240, A230, A220 (see Table II)). The error bars denote the accuracy of the positron lifetime measurement of ±3 ps. The lines are meant as eye guides.

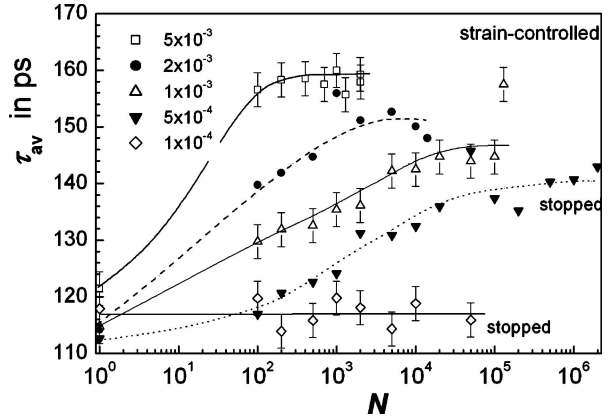

Figure 6 Evolution of the average positron lifetime τ_{av} with the number N of plastic strain-controlled load cycles for different applied plastic strain amplitudes ε_{pl} given in mm/mm (Experiments B5E3, A2E3, D1E3, C5E4, A1E4 (see Table III)). The error bars denote the accuracy of the positron lifetime measurement of ±3 ps. N denotes the number of load cycles. The lines are meant as eye guides.

data base available now, it could be confirmed that the scatter of $\tau_{av}(0)$ has no significant impact on the evolution of $\tau_{av}(N)$ and $\Delta\tau_{av}(N)$ during fatigue experiments.

In stress- and strain-controlled experiments a smallest deformation amplitude can be distinguished that has no significant effect on the average positron lifetime. This amplitude of 220 MPa, identified in the stress-controlled experiments, agrees well with the fatigue limit of 225 MPa [25]. The strain-controlled experiment with the lowest applied $\varepsilon_{pl} = 1 \times 10^{-4}$ did not yield any significant change of τ_{av} and was stopped after 50.000 cycles.

In stress- and strain-controlled experiments executed at values above the fatigue limit the average positron lifetime exhibits a pronounced increase during fatigue life. The higher the applied amplitude σ or ε_{pl} the higher is the increase rate $\Delta\tau_{av}/\Delta N$ during early fatigue life. A saturation-like behaviour can be recognized for $\tau_{av}(N)$. In stress-controlled experiments positron annihilation data are identical within the error margins after about 40% of fatigue life has been reached. Strain-controlled experiments show earlier saturation after about 10% of fatigue life.

For the highest applied stress amplitude of 290 MPa a positron lifetime of $\tau_{av}(N_f) = 178$ ps was determined at failure. This is significantly higher than the highest value of $\tau_{av} = 162$ ps registered in the strain-controlled experiment with $\varepsilon_{pl} = 5 \times 10^{-3}$ although stress amplitudes between 350 and 400 MPa have been determined from the hysteresis loops in this case. The stress amplitudes reached in the strain-controlled experiments in the range of $1 \times 10^{-4} \leq \varepsilon_{pl} \leq 5 \times 10^{-3}$ were between 212 MPa and about 400 MPa. This indicates a qualitatively and quantitatively different behaviour of the net defect-production in stress- and strain-controlled mode.

3.2. Reproducibility of experiments

The present investigation laid special emphasis on the reproducibility of the positron-lifetime measurements in view of its applicability for nondestructive testing. The different measurement campaigns contributing to the present results were performed with two different specimen geometries on three fatigue systems and with three ^{72}Se/^{72}As positron generators.

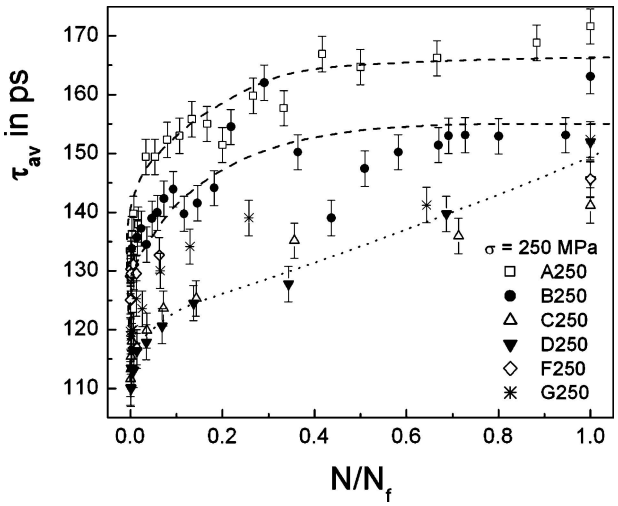

Figure 7 Evolution of the average positron lifetime τ_{av} in ps during stress-controlled fatigue experiments with a stress amplitude of σ = 250 MPa. The number of load cycles N has been normalized to the fatigue life of the specimens N_f. The experiments C250, D250 and G250 were performed on a testing systems that showed some alignment problems leading to premature failure of the specimens out of center of their gauge length. The eye guides refer to the specimens A250 and F250 with a fatigue life of 300300 and 802300 cycles, respectively.

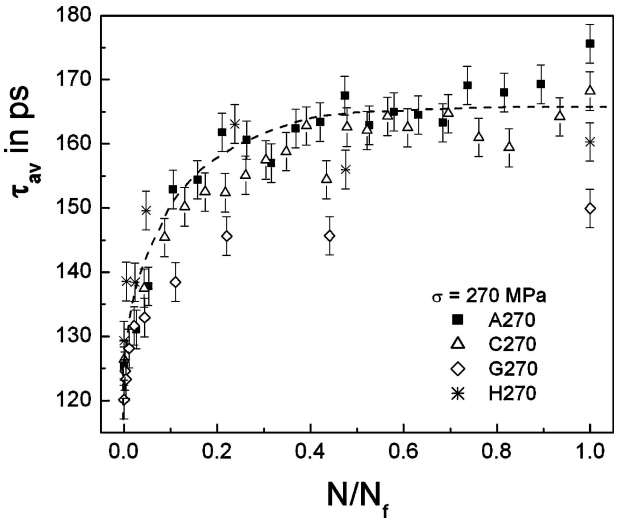

Figure 8 Evolution of the average positron lifetime τ_{av} in ps during stress-controlled fatigue experiments with a stress amplitude of σ = 270 MPa. The number of load cycles N has been normalized to the fatigue life of the specimens N_f. The eye guide refers to the experiments A270 and C270.

Figs 7 and 8 show the evolution of $\tau_{av}(N)$ for stress amplitudes of 250 and 270 MPa, respectively. The experiment F250 in Fig. 7 with the a low value of $\tau_{av}(N_f)$ at failure exhibited also the longest observed fatigue life of N_f = 802.300 and the smallest increase $\Delta\ \tau_{av}(N_f)$ until failure. The experiments C250 and D250 with similar fatigue life of N_f = 140.226 and N_f = 145.621, respectively, show a significantly less pronounced increase of τ_{av} with rather low values at failure ($\tau_{av}(N/N_f$ = 1)). Both specimens failed close to the radius at the end of the gauge length and not in its center region as usually. The same holds for specimen G250 that failed after only 77635 load cycles. These experiments and B260 were the only ones conducted on the MTS system 810 with 250 kN load capacity this indicates very likely an alignment problem that emphasized local fatigue

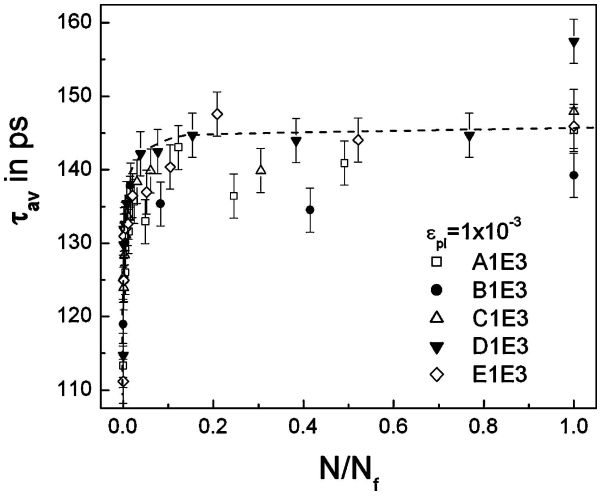

Figure 9 Evolution of the average positron lifetime τ_{av} in ps during strain-controlled fatigue experiments with a plastic strain amplitude of $\varepsilon_{pl} = 1 \times 10^{-3}$ mm/mm. The eye guide indicates the saturation of τ_{av} after about 10% lifetime.

around pre-existing surface flaws in a location outside the center region of the gauge length leading to premature failure. In these cases the positrons probed the development of fatigue-induced microstructure changes in a homogeneously loaded area whereas stress concentrations caused a locally higher loads and accelerated fatigue elsewhere leading to failure.

Fig. 8 presents a series of experiments carried out with a stress amplitude of 270 MPa. Again, specimen G270, with a smoother increase of $\tau_{av}(N)$ is accompanied by twice times longer fatigue life N_f.

In nearly all cases a different evolution of the average positron lifetime is related with a significantly different fatigue life N_f.

Fig. 9 shows the evolution of the average positron lifetime for the five experiments conducted at a plastic strain amplitude of $\varepsilon_{pl} = 1 \times 10^{-3}$. The scatter is less pronounced than in stress-controlled experiments. One eye guide describes the evolution sufficiently for the complete series of experiments. A saturation-like behaviour after about 10% of fatigue life can be recognized. The initial scatter of $\tau_{av}(0)$ is practically getting wiped out within the first 500 deformation cycles.

Practical applications were also hampered when a variation of the measurement site on the specimen surface would lead to significantly different values of τ_{av}. Therefore, on some specimens the measurements have been repeated varying the position of the source-detector assembly along the gauge length in steps of about 5 mm. Additionally some specimens have been rotated and the measurements have been repeated (180° for B2E3, 120° and 240° for B4E5). The variation of the measured average positron lifetimes was always within a range of at maximum ±3 ps.

3.3. The utility of positron annihilation for residual lifetime assessment

The scope of residual lifetime assessment is to determine at which percentage of lifetime a component is arrived. This requires the capability to relate a value measured during fatigue to the expected fatigue life. In the present case it is obvious that there is a pro-

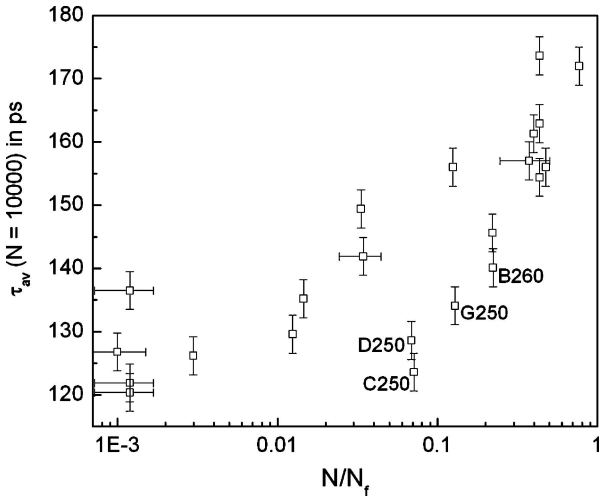

Figure 10 Relation between the the average positron lifetime $\tau_{av}(10000)$ measured after the first 10000 load cycles versus the normalized fatigue life N/N_f ($N = 10000$) in stress-controlled experiments. The experiments labelled C250, D250, G250, and B260 exhibited premature failure due to stress concentrations out of the center of the gauge length.

nounced increase of the average positron lifetime in the early stages of fatigue life and saturation is reached after about 40 and 10% in stress- and strain-controlled experiments, respectively.

Figs 10 and 11 present the average positron lifetime after 10000 and 1000 load cycles versus the normalized fatigue life N/N_f for stress- and strain-controlled experiments, respectively. The curves exhibit a linear increase of $\tau_{av}(N = 10000)$ and $\tau_{av}(N = 1000)$ with log N/N_f. The scatter is much more pronounced in the case of stress-controlled experiments. Since the fatigue life N_f exhibits an appreciable scatter under nominally identical load amplitudes it is only well-known for experiments conducted until failure. Nevertheless, Fig. 10 includes also data from experiments stopped before failure when a sufficient number of experiments was carried out until failure at the same stress amplitude and a meaningful standard deviation could be defined for $N_f(\sigma)$. These data can be recognized by the error bars given for log N/N_f. In Fig. 10 we assigned the specimen label to those experiments that fall significantly apart the overall tendency. It turns out that they have already been discussed in Section 3.2. for being failed at the border of the gauge length indicating local stress concentrations probably due to an alignment problem with the fatigue machine.

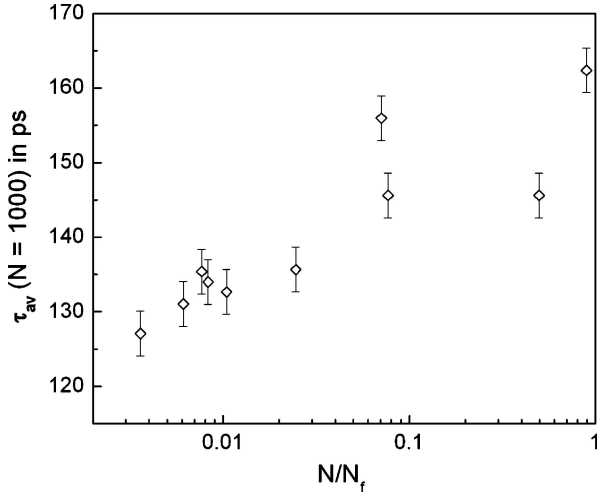

Figure 11 Relation between the average positron lifetime $\tau_{av}(1.000)$ measured after the first 1000 load cycles versus the normalized fatigue life N/N_f ($N = 1000$) in strain-controlled experiments.

4. Discussion

4.1. Comparison with other experimental investigations

Main scope of the present work was to examine the evolution of the average positron lifetime during stress- and strain-controlled fatigue experiments with emphasis on the reproducibility and the predictive power of positron lifetime measurements for nondestructive testing purposes. Concerning the large number of specimens tested and in the approach to follow each specimen until failure by positron lifetime measurements the present work differs from other work on steels presented by Kuramoto *et al.* [31] on Fe-0.5 wt% Si, by Karjalainen *et al.* [32] on mild steel by Gauster *et al.* [33] on stainless steel AISI 316 and more recently by Hartley *et al.* [20] and Asoka-Kumar *et al.* [34] on AISI 304, and by Bennewitz et al [35] on the stainless steel X6CrNiTi18-10 and on the carbon steel C45E.

Kawaguchi and different co-workers [13, 14, 16] reported on positron lifetime measurements and annihilation lineshape analysis in stainless steel AISI 316 L during stress- and total strain-controlled experiments. Positron lifetime measurements and positron annihilation lineshape analysis were carried out for stress- and strain-controlled tension-compression fatigue at amplitudes of $\sigma = 220$ MPa and $\varepsilon_{tot} = 3.1 \times 10^{-3}$, respectively [13]. Since Kawaguchi and Shirai controlled the total strain, comparison with the present experiments is not straight forward because because (i) $\varepsilon_{pl} < \varepsilon_{tot}$ and usually (ii) ε_{pl} is not constant throughout the experiments when ε_{tot} is kept constant. This may result in a different microstructure evolution.

Kawaguchi and Shirai [13] used 3 specimens to determine the typical fatigue life N_f for $\sigma = 220$ MPa and $\varepsilon_{tot} = 3.1 \times 10^{-3}$. Further specimens were cyclically deformed to 0.1, 1, 10, 25, 50, and 100% of this value. In contrary to the present work, positron annihilation measurements were performed on different specimens deformed to a different stage of fatigue life. This introduces an uncertainty concerning the real percentage of fatigue life. Moreover, Kawaguchi and Shirai [13] determined a fatigue life of $N_f = 357.000$ for their material at a stress amplitude of 220 MPa. In our material 220 MPa corresponds to the fatigue limit where 50% of the specimens reached $N = 10^7$ cycles without failure. We would expect $N_f = 357.000$ for $\sigma \approx 250$ MPa. Hence, the AISI 316 L used by Kawaguchi and Shirai [13] was in a microstructure state that made it more prone to fatigue failure than the material used for the experiments presented here. The reason could be a slightly different chemical composition, a longer thermal pretreatment and a different quenching rate achieved in the tube material as compared to the plates from which our specimens were prepared. In spite of these experimental differences, the results

of Kawaguchi and Shirai [13] confirmed the present findings, that the evolution of average positron lifetime proceeds faster in strain-controlled experiments than under stress control. Moreover, these authors convincingly demonstrated that the evolution of the average positron lifetime τ_{av} and that of the S-parameter are equivalent by plotting τ_{av} versus the parameter S that characterizes the annihilation line shape modified by Doppler broadening for specimens examined by both methods.

Asoka-Kumar *et al.* [34] examined two batches of stainless steel AISI 304 with different carbon content (0.056 and 0.014 at%). Like by Kawaguchi and Shirai [13] an average fatigue life was determined under the applied fatigue conditions (total strain control, $\varepsilon_{tot} = 6.6 \times 10^{-3}$) and then different specimens were cycled up to different stages in fatigue life. Positron lifetime was measured using a 2.8 MeV positron beam of Lawrence Livermore National Laboratory and the spectra were decomposed in a short (≈120 ps) and a long (≈220 ps) lifetime component. The long component was found to saturate after about 10% of fatigue life at an intensity of around 65–70%. Asoka-Kumar *et al.* [34] could identify carbon decorated small vacancy clusters as dominating trapping sites and moreover they could demonstrate by electron momentum studies that the carbon decoration of the trapping sites exhibits an evolution throughout fatigue life.

Karjalainen *et al.* [32] found a more gradual increase of the average positron lifetime during fatigue life on a mild steel (Fe-0.16% C-0.45%Mn). Their experiments were carried out in constant maximum stress cantilever bending and two identically deformed specimens were prepared in order to measure nondestructively the average positron lifetime in various stages of fatigue life by sandwiching a ^{22}Na-source between them. However, bending fatigue introduces a gradient of the stress amplitude from a maximum value at the surface to zero on the neutral line in the center of the specimen. Although the bending stress has been controlled in this case the positrons probe a volume subjected to different local stress and strain amplitudes. Therefore the results are difficult to compare with the present ones.

4.2. Reproducibility and predictive power

The present experiments show that the increase rate of the average positron lifetime until saturation is the most significant parameter related to the applied load amplitude. The value of the average positron lifetime at failure $\tau_{av}(N_f)$ is practically reached after 40 and 10% of fatigue life in stress- and strain-controlled experiments, respectively. The most simple evaluation of the initial increase in positron lifetime is the determination of $\tau_{av}(N)$ after $N = 10000$ or $N = 1000$ cycles, in most cases well before $\tau_{av}(N)$ saturates. In Figs 10 and 11 the mean positron lifetime measured after $N = 10000$ stress-controlled and $N = 1000$ strain-controlled load cycles are presented versus the normalized fatigue life N/N_f, respectively. Fig. 11 indicates that from a measurement of $\tau_{av}(N = 1000)$ it could be possible to estimate the fatigue life N_f as long as $\tau_{av}(N = 1000)$ is still below the saturation value for strain-controlled experiments. This is essentially the information needed for residual lifetime assessment. Also in strain-controlled experiments the tendency of $\tau_{av}(N = 10000)$ to increase with N/N_f is obvious however the data are subjected to a rather large scatter. In spite of being able to explain the deviation of the labelled data in Fig. 11 these data point to a further issue to be addressed for reliable lifetime estimates.

Positron annihilation provides a measurement on the integral amount of positron trapping sites in a certain rather small area whose location has to be chosen carefully. It cannot detect fatigue damage due local stress concentrations around pre-existing flaws elsewhere that might cause premature failure. Its strength is the very early assessment of fatigue-induced microstructure changes in homogeneous material that cannot be detected with any other nondestructive method without special specimen preparation. The issue of possible stress-concentrating inhomogeneities outside the observation area must be tackled in combination with less sensitive methods providing a larger visual field or by multiple measurements.

An interruption after exactly 10.000 and 1.000 cycles in stress- and strain-controlled experiments, respectively, seems only feasible in the laboratory. In practice this would mean that a reasonable guess for the number of load cycles were required to assess the length of the service period before testing. Values of $\tau_{av}(N)$ already in the saturation regime are no longer useful for residual lifetime assessments. They indicate however that the specimen passed already the first 10% or 40% of its fatigue life under strain- or stress-control, respectively.

On the other hand, in most practical cases, loading occurs with a statistical distribution of stress and stress rate and often with a mean stress unequal to zero, i.e., $\sigma_{min}/\sigma_{max} \neq -1$. Therefore, the aspect of loading with stress spectra and mean stress deserves special attention in future experiments.

For practical engineering applications it would therefore be an asset to combine positron annihilation with a second method that could distinguish between later stages of fatigue life when positron lifetime already saturated and to identify stress-concentrations that deserve special attention. From Tables II and III we can deduce a value of $\tau_{av} \approx 140$ ps as *alert level*. Below this value only one specimen failed. For higher average positron lifetimes the risk of failure becomes more and more imminent the higher τ_{av}. According to the knowledge of the authors there is no other method that could give so early alert on accumulating fatigue damage than positron annihilation without requiring cumbersome surface or specimen preparation.

Recently, Asoka-Kumar *et al.* [34] found evidence that in non heat-treated austenitic stainless steel AISI 304 the decoration of vacancies and small vacancy agglomerates exhibits a continuous evolution during fatigue life which is reflected in the Doppler broadening of the annihilation radiation. This could show the way to extend the application of positron annihilation beyond the saturation of τ_{av} by using more

refined methods of positron annihilation lineshape analysis.

4.3. Trapping sites in fatigued material

Fatigued materials contain a confusing variety of positron trapping sites. Most of them exhibit specific positron lifetimes within a range of typically 30–50 ps. So far there is no algorithm available that reliably could decompose an average positron lifetime in more than 3 components one of them being reserved for the source contribution. Moreover a reliable decomposition into 2 components with a lifetime difference of less than 50 ps would require recording at least $3 \cdot 10^6$ coincidence events [36]. These requirements counteract the attempts presented in the this paper to perform measurements with a mobile apparatus that is safe to handle for field applications obtaining results within reasonable time.

Table IV compiles some positron lifetime data available in literature for austenitic stainless steel, iron and nickel. In view of the grain size of around 40–50 μm in the present material, we neglect annihilation in grain boundaries since its statistical weight would be too small. The table is not exhaustive; e.g., there are neither experimental nor theoretical data available on the positron lifetime in jogs on dislocation lines as further supposed trapping sites [37]. The effect of lattice structure and carbon decoration on the theoretical positron lifetime in vacancies and small vacancy clusters has recently been treated by Asoka-Kumar *et al.* [34]. The reference given in the table refers to their experimental value on fatigued stainless steel AISI 304.

A comprehensive analysis of the individual contributions of all possible trapping sites would need to include also temperature dependent measurements since not all positron traps exhibit the same binding potential for positrons and thermal detrapping from shallow traps may occur (e.g. [44, 45]). Moreover, in view of the diffusion length of thermalized positrons under the present conditions that can be estimated to about 0.25 μm [28] and the inhomogeneous distribution of dislocations in patterns of alternating dense and poor regions with a typical separation of 1 to 2 μm, not all positrons will annihilate in the same environment. In face centered cubic metals, such as austenitic stainless steels, plastic strain may become localized in persistent slip bands (PSBs) where a dynamic equilibrium between defect production and annihilation is realized. These PSBs are embedded in a so-called matrix structure that deforms mainly elastically by a flip-flop motion of screw dislocations in the dislocation poor channels that separate veins with high dislocation density [6]. According to the model of Essmann, Gössele and Mughrabi [6] a diffusion flux of vacancies can be expected from the PSB regions into nearly unstrained matrix material. In such border regions between PSBs and matrix vacancy agglomerates may be formed that are protected from being segmented by moving dislocations. Therefore, a significant concentration of vacancy clusters could exist in a thin border stripe between PSBs and matrix.

A complete physical understanding of positron annihilation in fatigue microstructures is still a many years effort. The development of more sophisticated experimental methods for this purpose could benefit from accompanying temperature dependent positron annihilation measurements starting from very low temperatures with excellent statistics on very pure metals and the application of methods that allow a spatial resolution of positron annihilation in the micron range. Consequently, attempts to improve the spatial resolution of positron annihilation by developing positron "microbeams" [46] or positron "microscopes" [47] are very promising assets for basic fatigue studies and in support of nondestructive testing.

TABLE IV Compilation of positron lifetime data reported in literature for the annihilation in the perfect lattice and in various defects

Material	Annihilation site	Lifetime	Source
Iron	perfect lattice	105 ps	Dlubek *et al.* [38]
Iron	perfect lattice	110 ps	Kamimura *et al.* [39]
Nickel	perfect lattice	108 ps	Dlubek *et al.* [38]
AISI 304	perfect lattice	100 ps	Hartley *et al.* [20]
Iron/nickel	perfect lattice	104 ps	Staab *et al.* [36]
AISI 316	single vacancy	175 ps	Lopes Gil *et al.* [40]
Iron	single vacancy	175 ps	Dlubek *et al.* [38]
Nickel	single vacancy	180 ps	Dlubek *et al.* [38]
Iron	single vacancy	176 ps	Kamimura *et al.* [39]
Iron	single vacancy	175 ps	Vehanen *et al.* [41]
Iron	vacancy cluster	175–300 ps	Vehanen *et al.* [41]
AISI 304	divacancy	186 ps	Asoka-Kumar *et al.* [34]
AISI 304	3-vacancy	211 ps	Asoka-Kumar *et al.* [34]
AISI 304	4-vacancy	244 ps	Asoka-Kumar *et al.* [34]
Iron	dislocation	117 ps	Kuramoto *et al.* [42]
Iron	edge dislocation	165 ps	Park *et al.* [43]
Iron	screw dislocation	142 ps	Park *et al.* [43]
AISI 304	C-decorated vacancy cluster	220 ps	Asoka-Kumar [34]

5. Conclusions

The results presented demonstrate that positron annihilation is well suited for the detection of beginning fatigue damage and that it could be developed into a highly sensitive tool for nondestructive testing at least for single phase materials. The major findings agree well with those of Asoka-Kumar *et al.* [34] and of Kawaguchi with different co-workers [13–16]. Early measurements of the average positron lifetime exhibit a certain predictive power for residual lifetime estimates in laboratory experiments conducted at constant stress and strain amplitudes (cf. Figs 10, 11). However, real applications with components subjected to statistical distributions of stress and stress rate must be examined in order to verify whether the scatter of positron annihilation measurements can be tolerated. Recent findings of Asoka-Kumar *et al.* [34] indicating that the carbon decoration of small vacancy clusters is varying throughout fatigue life could show the way to extend the application of positron annihilation beyond the saturation of τ_{av} by using sophisticated methods of positron annihilation lineshape analysis.

In order to get further experience with the applicability of positron annihilation for fatigue damage evaluation the next steps have to consider experiments with a more complex fatigue history experimentally realized

by fatigue sequences with stress amplitude spectra and non-zero mean stress. Moreover, a survey on in-service components with reasonably well-known fatigue history or of samples prepared from failed components would be highly useful.

A. Appendix — Radiological safety

The irradiation of a Ge plate (2 mm thick, 10 mm in diameter) with 38 MeV alpha particles and the subsequent vapour deposition of the ^{72}Se has been performed with the Scanditronix MC40 cyclotron at our institute. The ^{72}Se/^{72}As positron generator with a maximum initial activity of about 25 μCi (0.9 MBq) caused a maximum dose rate of about 50 μSv/h in 1 cm distance from the source. On the base of the photo multiplier tube a maximum dose rate of 2 μSv/h has been measured. This site is important for handling the assembly. In 1 m distance from the load train with mounted positron generator the dose rate was 0.2 μSv/h. The dose rates decrease with the radioactive decay of the generator of about 8 days half-life. The dose rates indicate that there is no risk for the user under normal working conditions and the Health Physics authorized the use outside a controlled area. Since the initial activity was above the limits for free handling and the vulnerability of the assembly was not compatible with the definition of a sealed source, an area with a radius of 3 m around the load train of the fatigue machine has been declared as temporary surveillance area. Access was restricted to personnel directly involved in the experiments and a personal dosimeter was required. In order to avoid a smashing of the source in case of malfunction of the servohydraulic deformation system the cross-head of the deformation machine was lifted to a point that the totally expanded hydraulic actuator would leave enough space between the hydraulic grips to save the detector-source assembly.

References

1. J. D. ACHENBACH, *Int. J. Solids Struct.* **37** (2000) 13.
2. G. DOBMAN, N. MEYENDORF and E. SCHNEIDER, *Nucl. Eng. Design* **171** (1997) 95.
3. J. P. HIRTH and J. LOTHE, "Theory of Dislocations", 2nd ed. (Krieger Publishing Company, Malabar, Florida, USA, 1982).
4. S. SURESH, "Fatigue of Materials", 2nd ed. (Cambridge University Press, Cambridge, 1998).
5. U. ESSMANN and H. MUGHRABI, *Philos. Mag. A* **40** (1979) 731.
6. U. ESSMANN, U. GÖSSELE and H. MUGHRABI, *Philos. Mag.* **44** (1981) 405.
7. Z. S. BASINSKI and S. J. BASINSKI, *Acta Metall.* **37** (1989) 3275.
8. R. N. WEST, *Adv. Phys.* **XXII** (1973) 263.
9. R. M. NIEMINEN and M. J. MANNINEN, "Positrons in Solids" edited by P. Hautojärvi (Springer Series *Topics in Current Physics*) (Springer-Verlag, Berlin-Heidelberg-New York, 1979) p. 143.
10. P. J. SCHULZ and K. G. LYNN, *Rev. Mod. Phys.* **60** (1988) 701.
11. M. J. PUSKA and R. M. NIEMINEN, *ibid.* **66** (1994) 841.
12. S. HANSEN, U. HOLZWARTH, M. TONGBHOYAI, T. WIDER and K. MAIER, *Appl. Phys. A* **65** (1997) 47.
13. Y. KAWAGUCHI and Y. SHIRAI, *J. Nucl. Sci. Technol.* **39** (2002) 1033.
14. Y. KAWAGUCHI, N. NAKAMURA and S. YUSA, *J. Jpn. Inst. Met.* **66** (2002) 740.
15. *Idem.*, *Mater. Trans.* **43** (2002) 727.
16. Y. KAWAGUCHI and N. NAKAMURA, *J. Jpn. Inst. Met.* **65** (2001) 835.
17. B. SOMIESKI, R. KRAUSE-REHBERG, H. SALZ, and N. MEYENDORF, *J. Phys. IV* **5** (1995) C1–127.
18. M. T. HUTCHINGS, D. J. BUTTLE, R. COLBROOK, W. DALZELL and C. B. SCRUBY, *J. Phys. IV* **5** (1995) C1–111.
19. A. BARBIERI, S. HANSEN-ILZHÖFER, A. ILZHÖFER and U. HOLZWARTH, *Appl. Phys. Lett.* **77** (2000) 1911.
20. J. H. HARTLEY, R. H. HOWELL, P. ASOKA-KUMAR, P. A. STERNE, D. AKERS and A. DENISON, *Appl. Surf. Sci.* **149** (1999) 204.
21. M. GERLAND, J. MENDEZ, P. VIOLAN and B. AIT SAADI, *Mater. Sci. Engng.* **A118** (1989) 83.
22. K. OBRTLIK, T. KRUML and J. POLAK, *Mater. Sci. Engng.* **A187** (1994) 1.
23. Y. LI and C. LAIRD, *Mater. Sci. Engng.* **A186** (1994) 65 and 87.
24. Annual Book of ASTM Standards, Metals Test Methods and Analytical Procedures, vol. 03.01 (American Society for Testing and Materials, Philadelphia, PA, USA, 1992).
25. U. HOLZWARTH, H. STAMM, J. D. BOERMAN and S. COLPO, unpublished results (1994).
26. A. E. WALTAR and A. B. REYNOLDS, in "Fast Breeder Reactors" (Pergamon Press, New York, 1981).
27. T. M. WANG, B. Y. WANG, S. H. ZHANG and M. DOYAMA, *Mater. Sci. Forum* **105–110** (1992) 1321.
28. T. WIDER, S. HANSEN, U. HOLZWARTH and K. MAIER, *Phys. Rev. B* **57** (1998) 5126.
29. C. M. LEDERER and V. S. SHIRLEY (eds.), "Table of Isotopes" 7th edition (Wiley & Sons Inc., New York-Chichester-Brisbane-Toronto, 1978).
30. U. HOLZWARTH, A. BARBIERI, S. HANSEN-ILZHÖFER, P. SCHAAFF and M. HAAKS, *Appl. Phys. A* **73** (2001) 467.
31. E. KURAMOTO, V. NOVAK and V. PAIDAR, *Scripta Metall. Mater.* **26** (1992) 557.
32. L. P. KARJALAINEN, M. MOILANEN, R. MYLLYLÄ and K. PALOMÄKI, *Phys. Stat. Sol. (a)* **62** (1980) 597.
33. W. B. GAUSTER, W. R. WAMPLER, W. B. JONES and J. A. VAN DEN AVYLE, in Proceedings of the 5th International Conference on Positron Annihilation, Sendai, 1979, edited by R.R. Hasiguti and F. Fujiwara (Japan. Institute of Metals, Sendai, 1979) p. 125.
34. P. ASOKA-KUMAR, J. H. HARTLEY, R. W. HOWELL, P. A. STERNE, D. AKERS, V. SHAH and A. DENISON *Acta Mater.* **50** (2002) 1761.
35. K. BENNEWITZ, M. HAAKS, T. STAAB, S. EISENBERG, T. LAMPE and K. MAIER, *Z. Metallkde* **93** (2002) 778.
36. B. SOMIESKI, T. E. M. STAAB and R. KRAUSE-REHBERG, *Nucl. Instr. Meth. Phys. Res. A* **381** (1996) 128.
37. M. DOYAMA AND R. M. COTTERILL, in Proceedings of the 5th International Conference on Positron Annihilation, Sendai, 1979, edited by R. R. Hasiguti and F. Fujiwara (Japan. Institute of Metals, Sendai, 1979) p. 89.
38. G. DLUBEK, A. SOURKOV, S. DEPETASSE and N. MEYENDORF, in Proceedings of the 20th Risø International Symposium on Materials Science: Deformation Induced Microstructures: Analysis and Relation to Properties, edited by J. B. Bilde Sørensen, J. V. Carstensen, N. Hansen, D. Juul Jensen, T. Leffers, W. Pantleon, O. B. Pedersen and G. Winter (Risø National Laboratory, Roskilde, 1999) p. 305.
39. Y. KAMIMURA, T. TSUTSUMI and E. KURAMOTO, *J. Phys. Soc. Jpn.* **66** (1997) 3090.
40. C. LOPES GIL, A.P. DE LIMA, N. AYRES DE CAMPOS, P. SPERR, G. KÖGEL and W. TRIFTSHÄUSER, *Rad. Eff.* **112** (1990) 111.
41. A. VEHANEN, P. HAUTOJÄRVI, J. JOHANSSON, J. YLI-KAUPPILA and P. MOSER *Phys. Rev. B* **25** (1982) 762.
42. E. KURAMOTO, H. ABE, M. TAKENAKA, F. HORI, Y.

KAMIMURA, M. KIMURA and K. UENO, *J. Nucl. Mater.* **54** (1996) 239.
43. Y.-K. PARK, J. T. WABER, M. MESHII, C. L. SNEAD JR. and C. G. PARK, *Phys. Rev. B.* **34** (1986) 823.
44. K. PETERSEN, I. A. REPIN and G. TRUMPY, *J. Phys.: Condens. Matter* **8** (1996) 2815.
45. T. WIDER, K. MAIER and U. HOLZWARTH, *Phys. Rev. B* **60** (1999) 179.
46. H. GREIF, M. HAAKS, U. HOLZWARTH, U. MÄNNIG, M. TONGBHOYAI, T. WIDER, K. MAIER, J. BIHR and B. HUBER, *Appl. Phys. Lett.* **71** (1997) 2115.
47. A. DAVID, G. KÖGEL, P. SPERR and W. TRIFTSHÄUSER, *Phys. Rev. Lett.* **87** (2001) 67402.

Received 14 May 2004
and accepted 9 May 2005